

ORIGINAL ARTICLE

# Cellular interactions and gene expression analysis of two equine-derived bone graft materials: an *in vitro* study

Daniilo A. DI STEFANO<sup>1,2</sup>, Luca COCCOLUTO<sup>3,4</sup>,  
Paola PANINA-BORDIGNON<sup>3,4</sup>, Elena BRAMBILLA<sup>3,4</sup>, Francesca RUFFINI<sup>3,4</sup>,  
Valentina MURTAJ<sup>3,4</sup>, Francesco ORLANDO<sup>1,2</sup>, Matteo COLOMBO<sup>5</sup>, Christian FRIGERIO<sup>5</sup>,  
Anna DI BONA<sup>5</sup>, Daniele RECUPERO<sup>5</sup>, Marco MORRONI<sup>5\*</sup>, Enrico GHERLONE<sup>1,4</sup>

<sup>1</sup>Dental School, IRCCS San Raffaele Hospital, Vita-Salute University, Milan, Italy; <sup>2</sup>Private Practitioner, Milan, Italy; <sup>3</sup>Division of Neuroscience, IRCCS San Raffaele Scientific Institute, Milan, Italy; <sup>4</sup>Vita-Salute San Raffaele University, Milan, Italy; <sup>5</sup>Bioteck S.p.A., Arcugnano, Vicenza, Italy

\*Corresponding author: Marco Morroni, Bioteck S.p.A., via Enrico Fermi 49, 36057 Arcugnano, Vicenza, Italy.  
E-mail: [academy@bioteck.com](mailto:academy@bioteck.com)

*This is an open access article distributed under the terms of the Creative Commons CC BY-NC license which allows users to distribute, remix, adapt and build upon the manuscript, as long as this is not done for commercial purposes, the user gives appropriate credits to the original author(s) and the source (with a link to the formal publication through the relevant DOI), provides a link to the license and indicates if changes were made. Full details on the CC BY-NC 4.0 are available at <https://creativecommons.org/licenses/by-nc/4.0/>.*

## ABSTRACT

**BACKGROUND:** Bone grafting is a surgical procedure that involves the use of bone tissue or bone substitutes to repair damaged bone. In dentistry and maxillofacial surgery, bone graft substitutes from various sources are commonly used. Given their critical role in clinical outcomes, it is essential to thoroughly investigate the biological and mechanical properties of these materials.

**METHODS:** In this *in vitro* study, we evaluated the biological properties of two equine-derived bone graft substitutes in comparison to  $\beta$ -tricalcium phosphate. The materials included one equine-derived graft containing hydrolyzed type I collagen and another containing preserved type I collagen. To assess their biological performance, we analyzed cell viability, adhesion, osteogenic differentiation, and the expression of genes involved in bone remodeling.

**RESULTS:** All graft substitutes demonstrated similarly good biocompatibility. However, in the  $\beta$ -tricalcium phosphate group, intergranular tissue fibers or extracellular matrix were absent both before and after osteogenic differentiation. In contrast, cells cultured on the equine-derived graft containing hydrolyzed type I collagen exhibited intergranular tissue fibers and matrix, while those on the graft containing preserved type I collagen showed intergranular tissue fibers, individual cells, and matrix. Gene expression analysis suggested that  $\beta$ -tricalcium phosphate may undergo faster resorption kinetics compared to the equine-derived grafts, which were associated with gene expression patterns indicative of enhanced bone formation.

**CONCLUSIONS:** Our results suggest that both hydrolyzed and preserved type I collagen support bone matrix deposition more effectively than  $\beta$ -tricalcium phosphate, with preserved collagen demonstrating superior performance. From a clinical perspective, preserved collagen appears to be the optimal choice for larger or less contained bone defects, as it promotes faster cell repopulation and may lead to more rapid remodeling with the patient's own vital bone. In contrast, hydrolyzed collagen seems to elicit a slower cellular response and may be better suited for smaller, localized defects where immediate biological activity is less critical. Further research is essential to guide clinicians in selecting the most appropriate bone graft substitute based on the specific clinical context.

*(Cite this article as: Di Stefano DA, Coccoluto L, Panina-Bordignon P, Brambilla E, Ruffini F, Murtaj V, et al. Cellular interactions and gene expression analysis of two equine-derived bone graft materials: an *in vitro* study. Minerva Dent Oral Sci 2025;74:355-71. DOI: 10.23736/S2724-6329.25.05209-X)*

**KEY WORDS:** Heterografts; Biocompatible materials; Bone regeneration; *In vitro* techniques.

Significant bone loss can affect multiple bone segments as a result of tumors, traumatic injury, surgical procedures, disease, tooth loss, congenital anomalies, or other causes.<sup>1</sup> Although bone possesses remarkable regenerative capabilities, successful bone homeostasis depends on the presence of viable cells, adequate vascularization, growth factors, and a suitable extracellular matrix. When one or more of these elements are compromised, the natural process of bone repair may become insufficient. In such cases, bone grafting procedures are often employed to enhance bone regeneration and promote healing.<sup>2</sup>

Bone grafting is a surgical technique widely used in orthopedics, neurosurgery, and dental surgery, in which either autologous bone tissue or bone substitute materials are used to repair and reconstruct diseased or damaged bone. The primary goals of bone grafts are to provide mechanical support and to stimulate bone regeneration, ultimately leading to the replacement of the graft with new, functional bone.<sup>3</sup> Over the past decade, the use of bone grafts has become increasingly important in dentistry – not only to correct functional deficits but also to meet aesthetic demands that significantly impact patients' quality of life.

Therefore, there is a growing need for graft materials with specific biological and mechanical characteristics tailored to various dental applications. Bone healing at the graft site occurs via one or more biological mechanisms: osteoconduction, osteoinduction, and osteogenesis.<sup>4</sup> Osteoconduction refers to the ability of a graft to provide a bioactive scaffold that supports the attachment and growth of host cells, allowing new bone to form along its surface.<sup>5</sup> Osteoinduction involves the recruitment of host stem cells to the graft site, where local signaling proteins induce their differentiation into osteoblasts that synthesize new bone.<sup>6</sup> Osteogenesis, on the other hand, describes the direct formation of bone by viable osteoblasts or progenitor cells contained within the graft material itself.<sup>5, 7</sup>

Bone grafts can be classified into several categories: autografts, allografts, xenografts, synthetic materials, and various combinations thereof. Autografts, which are harvested from the patient's own body, are considered the gold stan-

dard among grafting materials due to their intrinsic osteogenic properties. Because they originate from the same individual, autografts carry the lowest risk of immunogenicity and histocompatibility issues. However, they are associated with several drawbacks, including donor site morbidity and increased surgical risk due to the additional procedure required for bone harvesting – complications may include bleeding, infection, inflammation, and postoperative pain.<sup>6, 8</sup>

Allogeneic grafts (or allografts) are derived from a donor of the same species, either from a living individual or processed cadaveric bone. Processing is necessary to minimize immune reactions and prevent the transmission of infectious diseases.<sup>9</sup> Allografts are osteoconductive and osteoinductive, but lack osteogenic potential, and their biological and mechanical integrity can be diminished during processing. Nonetheless, they are frequently preferred over autografts due to the elimination of donor site morbidity and the reduced need for an additional surgical procedure. Despite these advantages, allografts are associated with high processing costs, batch-to-batch variability, limited availability, risk of disease transmission, immune rejection, and potential cultural or religious concerns.<sup>10-12</sup>

Xenografts originate from species genetically unrelated to the host. Their osteoconductive properties are primarily due to their inorganic structure, which consists mainly of hydroxyapatite. Xenografts can be derived from various sources, including cattle, pigs, horses, coral exoskeletons, and eggshells.<sup>13-15</sup> One of the main advantages of xenografts is the similarity of their inorganic chemical composition and morphological structure to that of human bone.<sup>13</sup> However, their primary disadvantages include the loss of osteoinductive potential and possible physico-chemical alterations to the inorganic component during processing, which is necessary to eliminate antigenicity.<sup>16</sup> Additional concerns involve the theoretical residual risk of disease transmission, necessitating rigorous validation of processing methods to ensure inactivation and removal of viruses and prions (especially for bovine-derived materials), as well as potential religious objections.<sup>11, 17</sup> Despite these challenges, various xenografts have been developed and are currently in clinical use.<sup>18-21</sup>

To address the potential immunogenicity and donor site morbidity associated with autografts, artificial synthetic bone substitutes have been developed to closely mimic the biological properties of natural bone. Synthetic materials offer several advantages over autogenous, allogeneic, or xenogeneic grafts: they are widely available due to ease of manufacturing and carry no risk of disease transmission.<sup>22</sup> However, currently available synthetic substitutes generally possess only osteoconductive properties, and their morphological structure often differs significantly from that of human trabecular bone. Examples of synthetic materials include calcium phosphate compounds such as hydroxyapatite and  $\beta$ -tricalcium phosphate ( $\beta$ -TCP), ceramics, bioglasses, metals like nickel-titanium, and various polymers.

Among these options, xenografts containing type I collagen – produced by enzymatically processing horse bone to remove antigenicity – represent a valuable compromise with demonstrated efficacy in diverse clinical settings.<sup>23-28</sup> The preservation of native collagen structure provides sufficient mechanical strength to support fixation using osteosynthesis devices, which is essential in major dental surgical procedures such as large bone augmentations using bone blocks, as well as in orthopedic and neurosurgical applications.<sup>11, 29, 30</sup> Furthermore, these collagen-containing xenografts have been associated with a greater amount of newly formed bone compared to collagen-free substitutes, as demonstrated in both preclinical<sup>31, 32</sup> and clinical studies, with favorable outcomes reported in oral surgery<sup>33-35</sup> and other fields.<sup>23-26</sup>

Despite these promising findings, to the best of the authors' knowledge, a comprehensive *in vitro* evaluation comparing the properties of bone graft substitutes containing either denatured (hydrolyzed) or native type I collagen is still lacking. Therefore, investigating the molecular-level differences is crucial – particularly when contrasting preserved collagen in its native, large, and complex molecular form with hydrolyzed collagen, which consists of smaller peptide fragments. Each fragment may have a distinct chain structure, and some peptides could be lost during manufacturing. Understanding these differences is essential to assess their behavior and potential clinical applications.

Moreover, to optimize patient outcomes, the *in vitro* characterization of bone graft materials plays a crucial role in guiding clinical decision-making and facilitating the selection of biomaterials tailored to the specific requirements of the surgical site, bone condition, and type of procedure (e.g., bone repair, reconstruction, or augmentation).

To address this need, the aim of the present study was to evaluate the *in vitro* properties of two equine-derived bone grafts – one containing hydrolyzed type I collagen (EBHC) and the other containing preserved type I collagen (EBPC) – using a collagen-free synthetic bone substitute,  $\beta$ -tricalcium phosphate ( $\beta$ -TCP), as the control material.

## Materials and methods

The researchers' expertise in biology, regenerative medicine, and molecular biology, combined with their previous work in stem cell research and gene expression analysis, is highly relevant to this study. Collaboration with specialists and industry professionals facilitated access to essential materials, further strengthening the research foundation. Additionally, the team's comprehensive understanding of cell biology positively influenced the experimental design and data interpretation, ensuring methodological rigor and scientific relevance. Conducted in a regulated laboratory setting, the study employed RT-qPCR and immunohistochemistry to evaluate gene expression and cellular interactions, adhering to ethical and technical scientific standards. However, further analyses should be conducted to expand the scope of the research and validate the findings under different experimental conditions. The multidisciplinary approach ensured rigorous, clinically relevant results that support the use of equine-derived materials in regenerative medicine.

### Biomaterials

EBHC (BIO-GEN<sup>®</sup>, Bioteck S.p.A., Arcugnano, Italy) and EBPC (OSTEOPLANT<sup>®</sup>, Bioteck S.p.A., Arcugnano, Italy) are produced using the patented Zymo-Teck<sup>®</sup> process, which starts from equine bone. This process employs a specific set

of enzymes that operate in an aqueous environment at low temperature. Under these conditions, the original equine tissue is effectively deantigenated, resulting in a biocompatible material.

The use of low temperatures preserves the mineral component of the bone entirely. Furthermore, by adjusting the enzymatic activity within the Zymo-Teck® process, it is possible to either preserve the native bone collagen (EBPC) or partially degrade the collagen (EBHC). In this study, cancellous granules of EBHC (BGS-20, 0.25-1 mm) and EBPC (OSP-OX38, 0.25-1 mm) were utilized.  $\beta$ -TCP (TCP Dental, porous granules 0.5-1 mm, Kasios, L'Union, France), a widely used synthetic bone substitute,<sup>36</sup> was included in all experiments as the control material.

To standardize and quantify the amount of biomaterial used in the experiments, the granules were weighed, and the average weight corresponding to the amount uniformly covering the bottom of a well in a 96-well plate was calculated. Five measurements were taken for each biomaterial, resulting in average weights of 4.5 mg/well for EBHC, 9.5 mg/well for  $\beta$ -TCP, and 6.5 mg/well for EBPC.

### Cell line

All experiments were conducted using the 143B cell line (ATCC-CRL-8303). The 143B osteosarcoma cell line was chosen as a model due to its high osteoblastic activity and relevance in studying bone metabolism and regeneration, despite its tumor origin, which may not fully replicate the physiology of normal osteoblasts.

Cells were cultured adherently in complete Eagle's Minimum Essential Medium (EMEM) supplemented with 0.015 mg/mL 5-bromo-2'-deoxyuridine (B5002, 90%) and 10% fetal bovine serum (FBS). Upon reaching confluency, the culture medium was removed, and cells were rinsed with a solution containing 0.25% trypsin and 0.02% EDTA, then incubated at room temperature for approximately 10 minutes to facilitate detachment. Fresh medium was added to stop the enzymatic reaction, and cells were transferred to new flasks. The medium was refreshed two to three times per week.

For each experiment, wells were pre-filled with minimal medium 24 hours before seeding

and incubated for 1 hour to stabilize temperature and CO<sub>2</sub> levels. Biomaterials were then added to each well. The cell density was optimized at 3000 cells per mg of biomaterial, with cells suspended in 200  $\mu$ l of culture medium for seeding.

### Histological staining

The following reagents were used to evaluate cell adhesion and differentiation on the scaffolds: Crystal Violet (CV, Sigma-Aldrich V5265) for protein staining, Von Kossa (VK, Sigma-Aldrich 100362), a calcium stain, and Nuclear Fast Red (NFR, Sigma-Aldrich N8002) for DNA staining. For CV staining, biomaterials were incubated with 0.4% and 0.04% CV in distilled water for 5 minutes at RT. After removal of CV, the biomaterials were washed five times with distilled water for 5 minutes each time. For VK staining, biomaterials were incubated with 1% silver nitrate, previously filtered with a 0.8  $\mu$ m filter, incubated under a UV lamp for 30 minutes and then washed three times at RT. For NFR staining, biomaterials were incubated with NFR 0.1% and 0.02% in distilled water for 5 minutes at RT, and after removing NFR, the biomaterials were washed five times with distilled water for 5 minutes each. Finally, as regards VK+NFR staining (VK 1% + NFR 0.02%), VK staining was performed as described above, NFR 0.02% was added for 5 minutes at RT and then washed five times quickly with distilled water.

After staining, all samples were air-dried for at least 18 hours and then analyzed using the Axiozoom V16 microscope (Zeiss) in the Applied Microscopy Laboratory at Tecnopolo Mario Veronesi (TPM, Mirandola, MO) with a 1.5x objective and 50x digital magnification. Images were acquired with Zen Pro software (Zeiss) using the Z-stack plugin. Samples with low dye absorbance were re-analyzed at 100x digital magnification. All images were acquired and analyzed in a blinded manner.

### Cell viability

To assess cell viability on the scaffolds, the Live and Dead assay for mammalian cells (Thermo-scientific, L3224) was used. On the 10th day after seeding the cells onto the scaffolds, the supernatant was discarded, the cells were rinsed with

100  $\mu$ l PBS 1X and incubated with a solution of 0.05% calcein and 0.2% di-ethidium bromide in PBS 1X at 37 °C and 5% carbon dioxide for 45 minutes. The solution was then removed and the cultures were washed in PBS 1X for 5 minutes at RT and analyzed histologically with AxioZoom V16 (Zeiss) as described above.

### Osteogenic differentiation

Cells were plated together with biomaterials in MW96 round-bottom or flat-bottom plates with low adhesion, using both complete Eagle's Minimum Essential Medium in Earle's BSS and differentiation medium. The differentiation medium consisted of complete medium supplemented with 50  $\mu$ M ascorbic acid (Sigma-Aldrich A4403), 10 mM  $\beta$ -glycerophosphate (CABRU 14405), and 10 nM dexamethasone (Sigma-Aldrich D1756). The medium was changed every other day. FBS and phenol red were removed in the last medium change before colorimetric assays. Cells were maintained in medium for 3 weeks and analyzed by imaging on day 17.

### Quantitative gene expression analysis

PCR analysis was performed on day 17 on RNA extracted from cells grown in the differentiation medium assay. Total RNA was isolated using the RNeasy Mini Kit (Qiagen #74104) according to the manufacturer's instructions. RNA samples were eluted from the columns with 30  $\mu$ l of RNase-free water, and concentrations were determined spectrophotometrically using the A260 (Nanodrop-ND1000). Semi-quantitative RT-PCR was conducted using pre-developed TaqMan™ assay reagents on a QuantStudio 3 Real-Time PCR System (Thermo Fisher) following the manufacturer's protocol. cDNA was synthesized from 500 ng total RNA using the ThermoScript IV RT-PCR system (Thermo Fisher). Two hundred ng of cDNA was used for RT-PCR with the following ready-made TaqMan® Gene Expression Assays (Thermo Fisher): RUNX2 (HS01047973\_m1), TNFRSF11A (RANK) (HS00921372\_m1), ALPL (HS01029144\_m1), SPP1 (OSTEOPONTIN) (HS00959010\_m1), COL1A1 (HS00164004\_m1), BGLAP (OSTEOCALCIN) (HS01587813\_g1), and GAPDH

(HS99999905\_m1). Data were acquired using Thermo Fisher Connect™ software with spectral compensation and analyzed using the threshold cycle (CT) relative quantification method. GAPDH was used as the housekeeping gene. Three samples per experimental group were analyzed: differentiated +  $\beta$ -TCP, differentiated + EBHC, and differentiated + EBPC. A one-way ANOVA followed by Dunnett's post-hoc test was performed to compare EBHC with  $\beta$ -TCP and EBPC with  $\beta$ -TCP. All data are expressed as mean $\pm$ SEM.

Due to the complexity of the differentiation protocol and the limited yield of cells, performing additional replicates was not feasible, especially given the multiple analyses conducted on the same cell cultures. Nonetheless, three biological replicates were included, which is generally considered sufficient for statistical analysis and interpretation.

## Results

### Cell viability

To evaluate cell viability on the scaffolds under investigation (EBHC, EBPC, and  $\beta$ -TCP), a live/dead cell assay was performed on day 10 after seeding (Figure 1, 2, 3). Six replicates were analyzed for each cell-scaffold combination, with two empty scaffold replicates included as negative controls. Confirming the biocompatibility of all tested materials, a marked prevalence of viable cells was observed on all colonized scaffolds (green cells in Figure 1, 2, 3). Moreover, very few dead cells were detected in all samples (red cells in Figure 1, 2, 3), and no signal was observed on empty scaffolds (data not shown).

### Cell adhesion

To evaluate cell adhesion on the three scaffolds, 1500, 3000, or 6000 cells/mg scaffold were seeded and analyzed at 3 and 10 days after seeding by staining with 0.04% Crystal Violet (CV) (Figure 4, 5, 6). Six replicates were tested for each condition, and the following elements were considered in the analysis: 1) single cells to evaluate scaffold biocompatibility based on cell morphology;

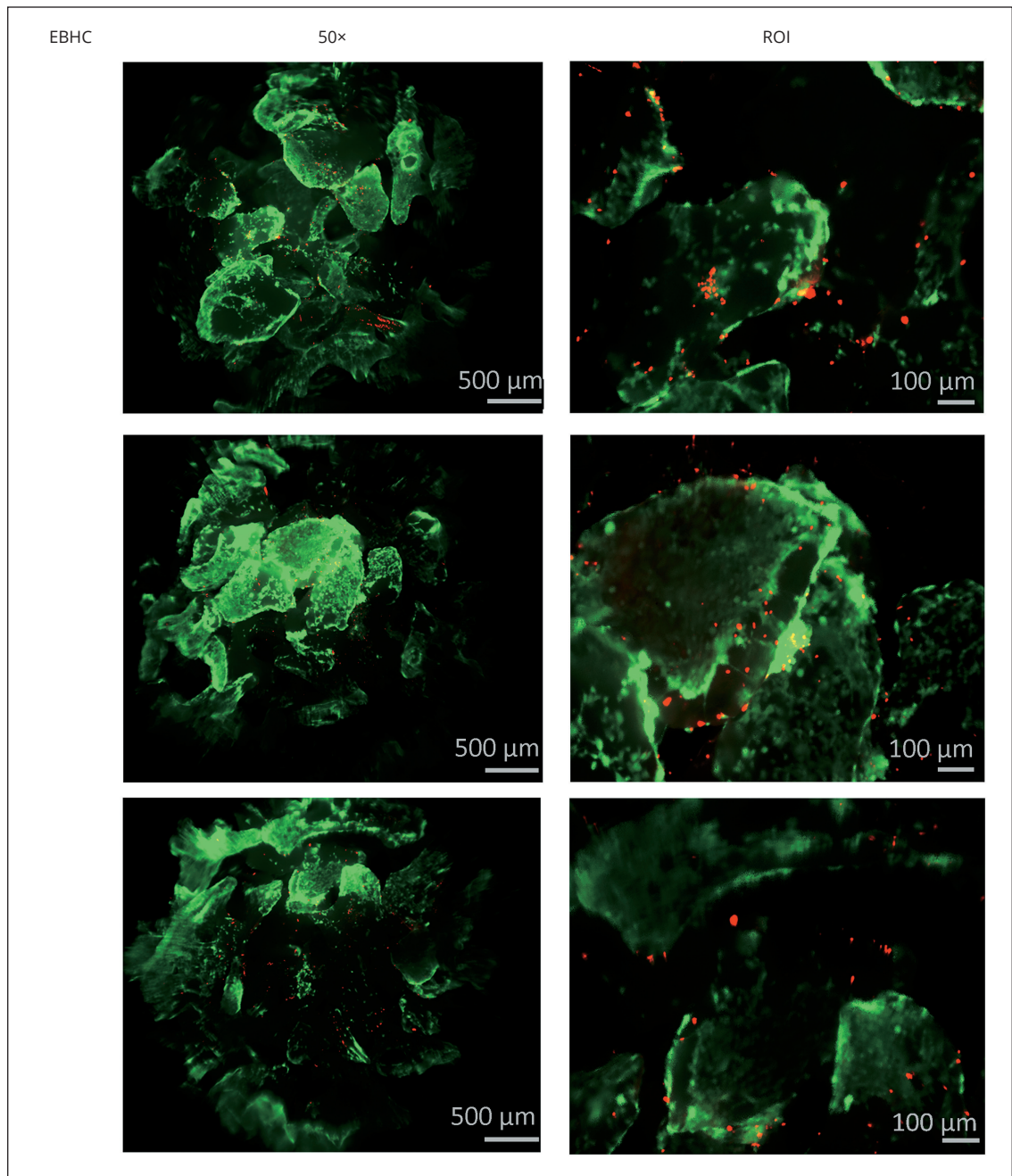


Figure 1.—EBHC demonstrated biocompatibility on 143B cells. Live and Dead assay was performed on fresh 3D cultures on day 10 after seeding. Viable cells are marked in green, while dead cells are marked in red. Images were acquired using the AxioZoom V16 microscope with a 15x objective and 50x magnification. Scale bar ROI=100  $\mu$ m.

2) tissue areas covering the scaffold, indicating scaffold colonization; 3) presence of tissue fibers between the scaffold granules, indicating colonization through compaction of the granule struc-

ture. The experiment showed that cells adhered to all scaffolds, although some differences were observed. At both time points, cells on EBHC formed tissue fibers spreading between the gran-

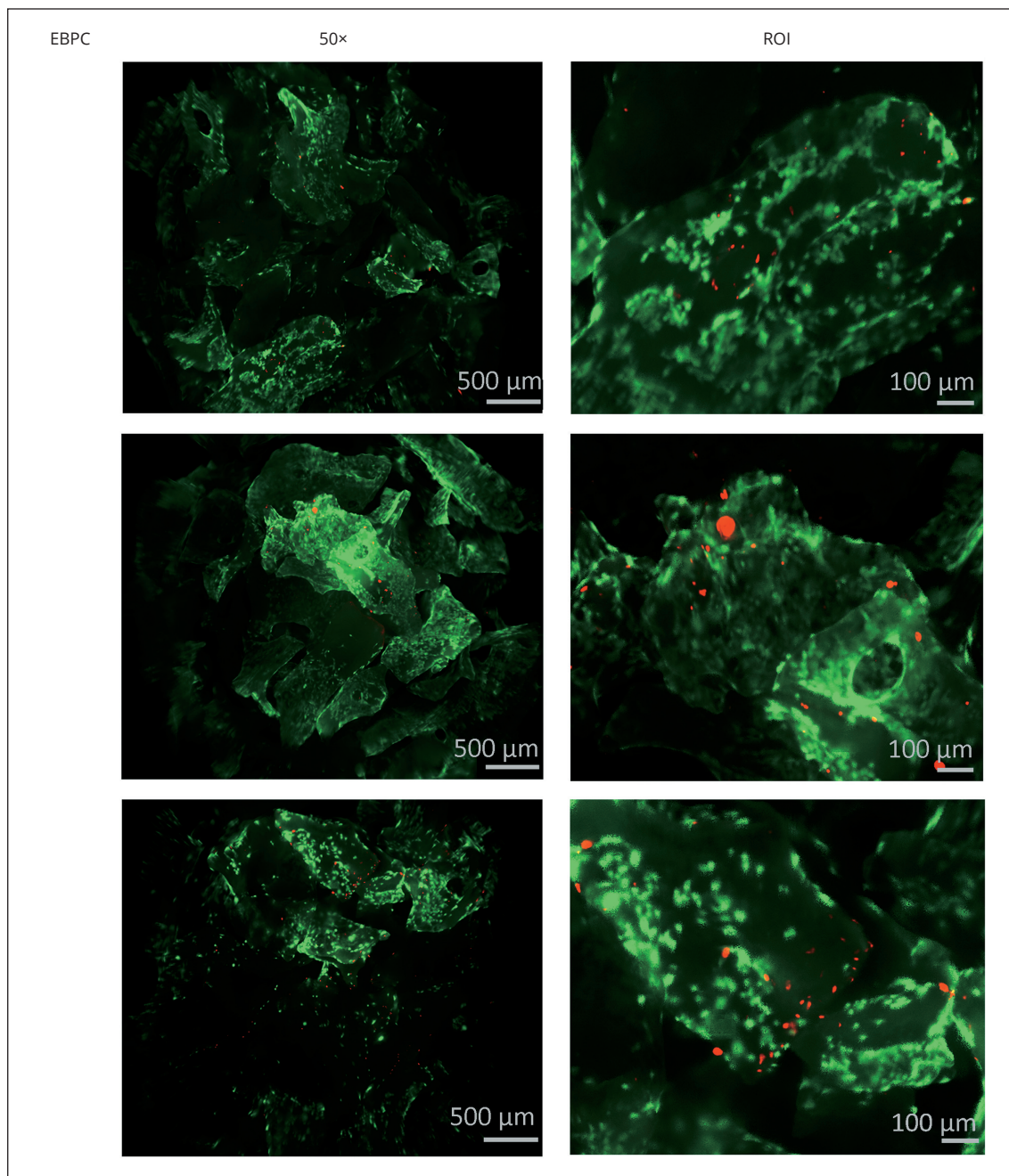


Figure 2.—EBPC demonstrated biocompatibility on 143B cells. Live and Dead assay was performed on fresh 3D cultures on day 10 after seeding. Viable cells are marked in green, while dead cells are marked in red. Images were acquired with the AxioZoom V16 microscope, using a 15x objective and 50x magnification. Scale bar ROI=100  $\mu$ m.

ules. On EBPC, single cells were seen on day 3, which developed into a compact layer covering the scaffold by day 10. A dose-dependent colonization was observed with EBHC, but not with

EBPC. On  $\beta$ -TCP, only single cells were observed at both time points, indicating very limited colonization even when seeding higher cell concentrations.

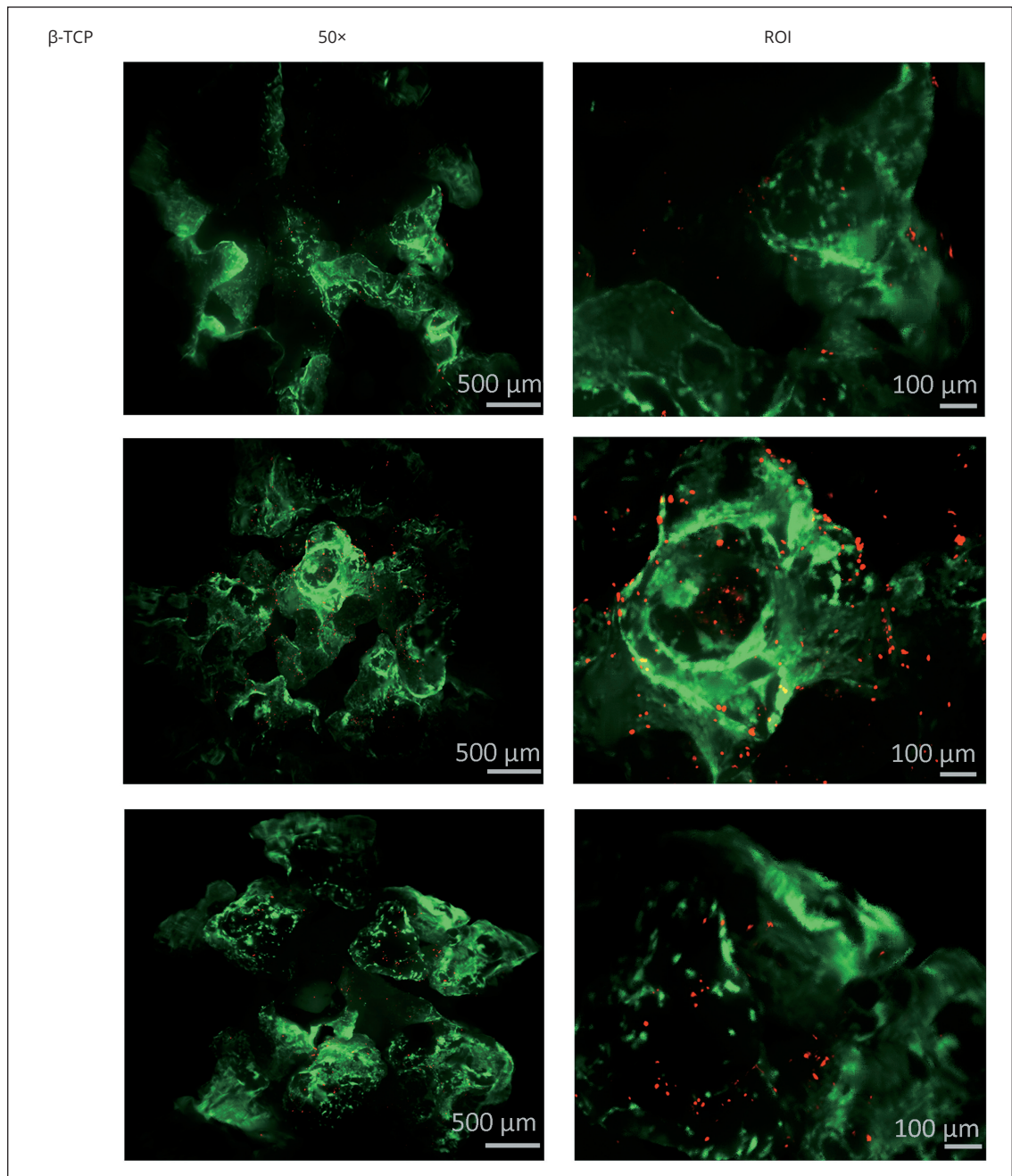


Figure 3.— $\beta$ -TCP demonstrated biocompatibility on 143B cells. Live and Dead assay was performed on fresh 3D cultures on day 10 after seeding. Viable cells are marked in green, while dead cells in red. Images were acquired with AxioZoom V16, objective 15x, magnification 50X. Scale bar ROI=100  $\mu$ m.

### Osteogenic differentiation

Osteogenic cell differentiation on the three scaffolds was assessed 17 days after incubation by

staining with 0.1% VK/0.02% NFR (Figure 7, 8, 9). Scaffolds seeded with both induced and non-induced cells were analyzed. ROIs obtained by digital magnification allowed visualization of

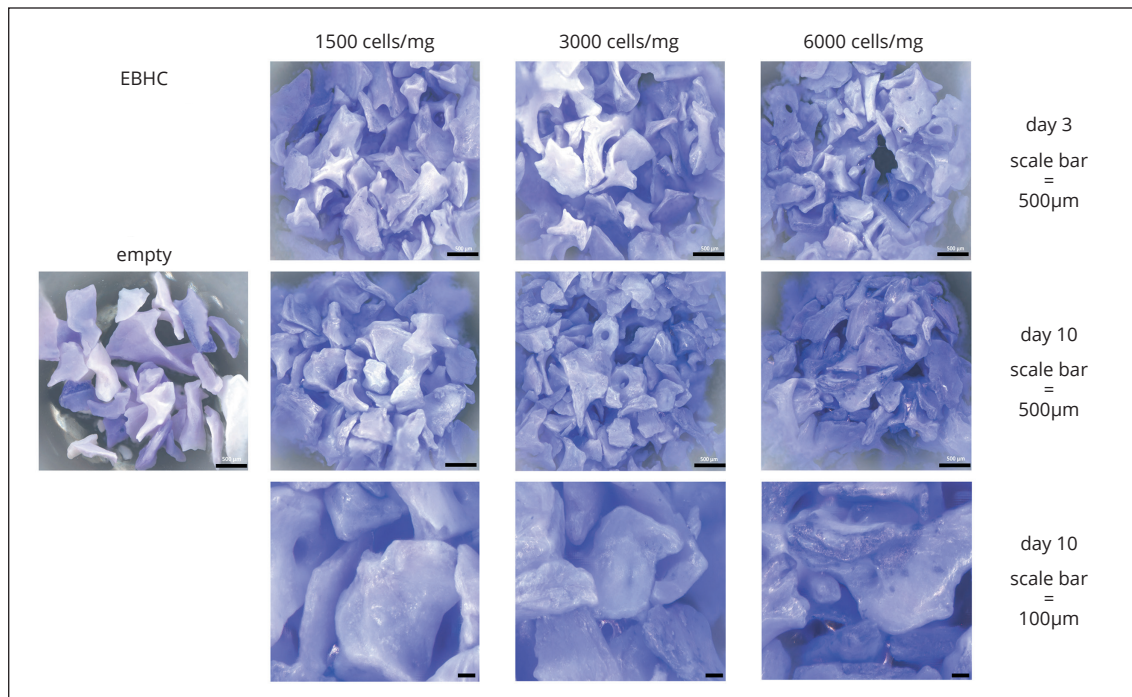


Figure 4.—Adhesion of 143B cells on EBHC resulted in dose-dependent colonization. Cells were seeded at concentrations of 1500, 3000, and 6000 cells/mg of scaffold. 3D cultures were fixed on days 3 and 10 after seeding and stained with 0.04% CV. Images were acquired using the AxioZoom V16 microscope with a 15x objective and 50x magnification. Scale bar ROI=100 µm.

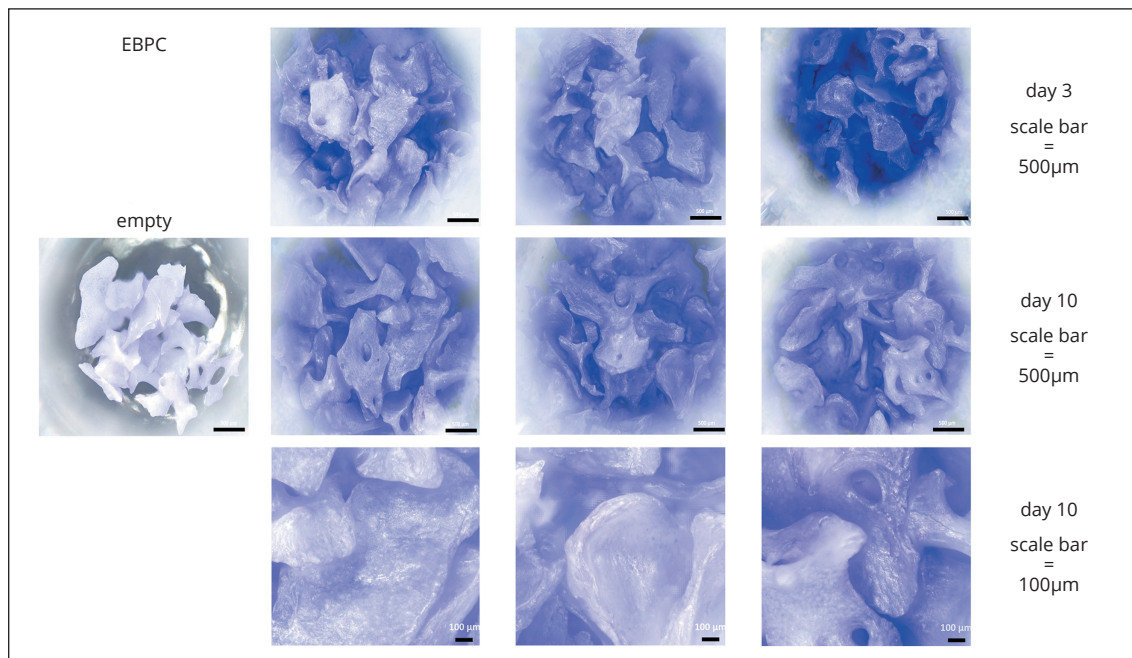


Figure 5.—Adhesion of 143B cells on EBPC generated a compact layer. Cells were seeded at concentrations of 1500, 3000, and 6000 cells/mg of scaffold. Three-dimensional (3D) cultures were fixed on days 3 and 10 after seeding and stained with 0.04% CV. Images were acquired using the AxioZoom V16 microscope with a 15x objective and 50x magnification. Scale bar ROI=100 µm.

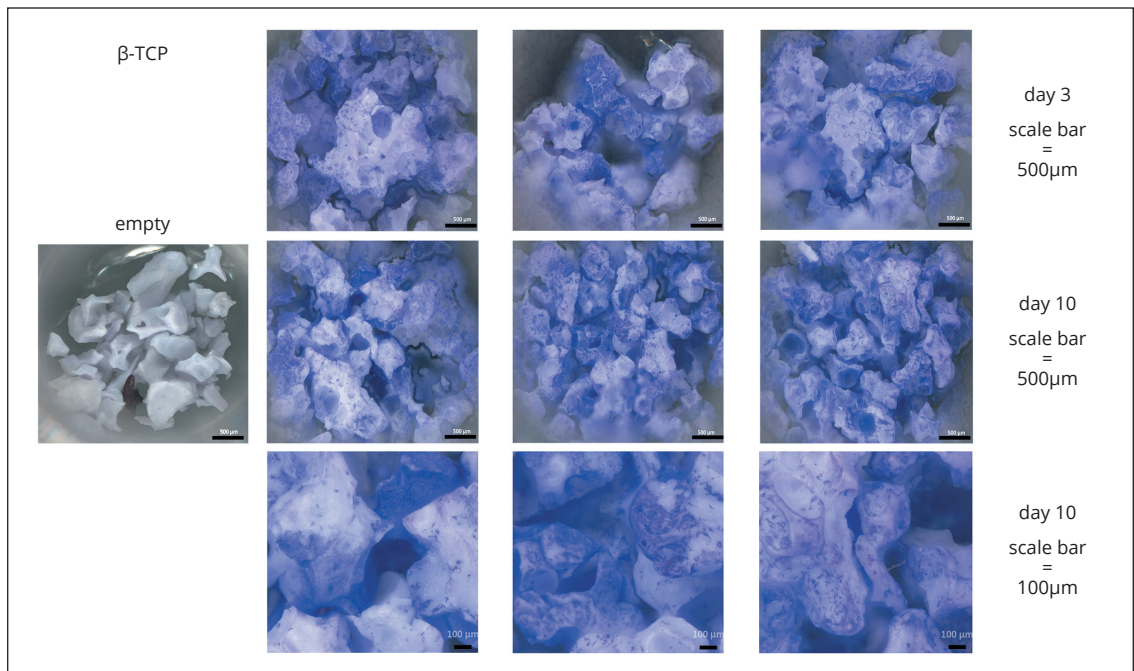
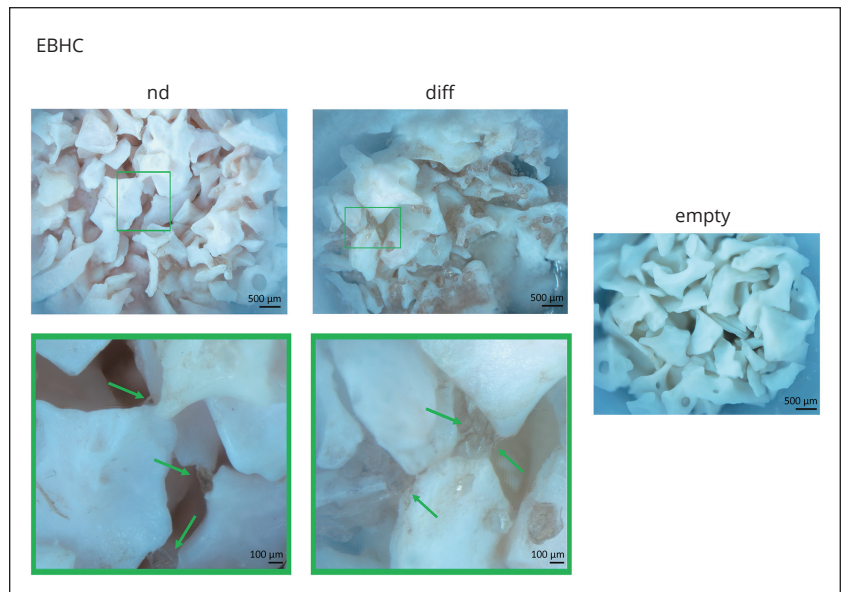


Figure 6.—Adhesion of 143B cells on  $\beta$ -TCP generated very limited colonization. Cells were seeded at concentrations of 1500, 3000, and 6000 cells/mg scaffolds. 3D cultures were fixed on day 3 and day 10 after seeding and stained with 0.04% CV. The images were acquired with AxioZoom V16, objective 15x, magnification 50X. Scale bar ROI=100  $\mu$ m.

intergranular tissue structures (green arrows in Figure 7, 8, 9) and/or VK-positive deposits (red arrows in Figure 7, 8, 9). NFR-positive tissue fibers were observed in EBHC samples under both

induced and non-induced conditions, while no VK-positive deposits were detected (Figure 7). NFR-positive tissue fibers, as well as VK-positive deposits, were observed in EBPC samples

Figure 7.—A predominance of tissue fibers was observed on EBHC. Osteogenic differentiation of 143B cells on EBHC assessed at 17 days after the induction of differentiation. 3D cultures were stained with VK 0.1%/NFR 0.02%. Tissue fibers are indicated with green arrows, while matrix deposition areas are not detected. The images were acquired with AxioZoom V16, objective 15x, magnification 50X. Scale bar ROI=100  $\mu$ m (colors in the online version).



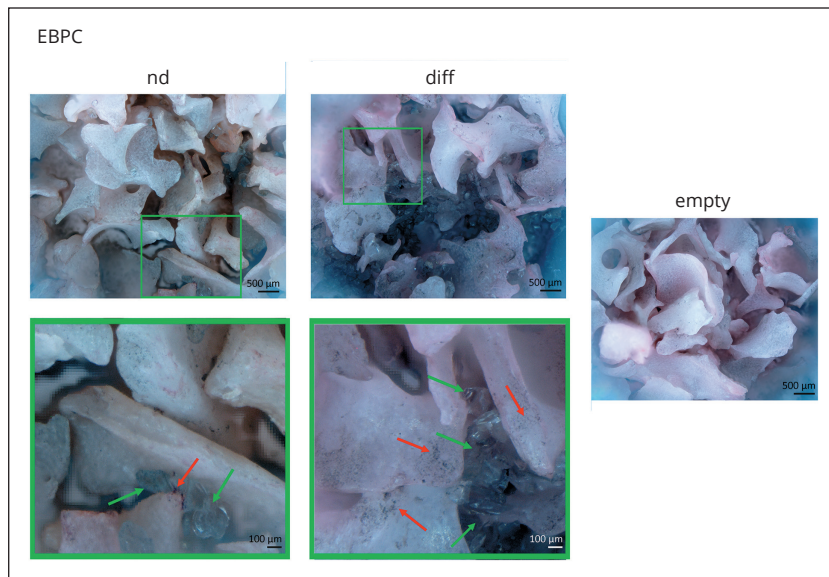


Figure 8.—Tissue fibers and matrix deposition were detected on EBPC. Osteogenic differentiation of 143B cells on EBPC was assessed at 17 days after the induction of differentiation. 3D cultures were stained with VK 0.1%/NFR 0.02%. Tissue fibers are indicated with green arrows, while matrix deposition areas are indicated with red arrows. The images were acquired with AxioZoom V16, objective 15x, magnification 50X. Scale bar ROI=100  $\mu$ m (colors in the online version).

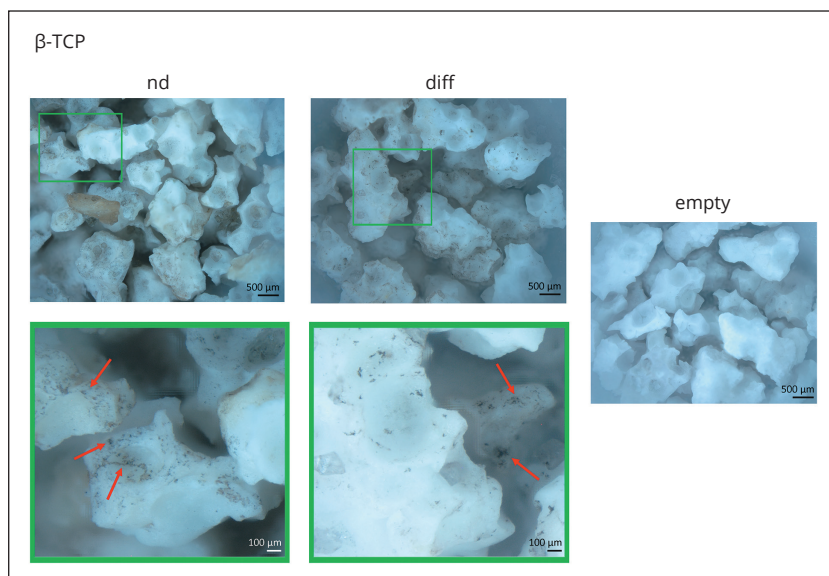


Figure 9.—A minimal presence of matrix deposition was observed on  $\beta$ -TCP. Osteogenic differentiation of 143B cells on  $\beta$ -TCP was assessed 17 days after the induction of differentiation. 3D cultures were stained with VK 0.1%/NFR 0.02%. Matrix deposition areas are indicated with red arrows; no tissue fibers were detected. Images were acquired with AxioZoom V16, objective 15x, magnification 50X. Scale bar ROI=100  $\mu$ m (colors in the online version).

under both conditions, with stronger NFR and VK positivity in the induced sample (Figure 8).  $\beta$ -TCP samples showed absence of tissue fibers and weak VK positivity, with similar signals in induced and non-induced samples (Figure 9). Empty scaffolds showed no signal. The different elements – single cells, intergranular tissue fibers, and tissue covering the scaffold surface – observed on the three scaffolds are summarized in Table I.

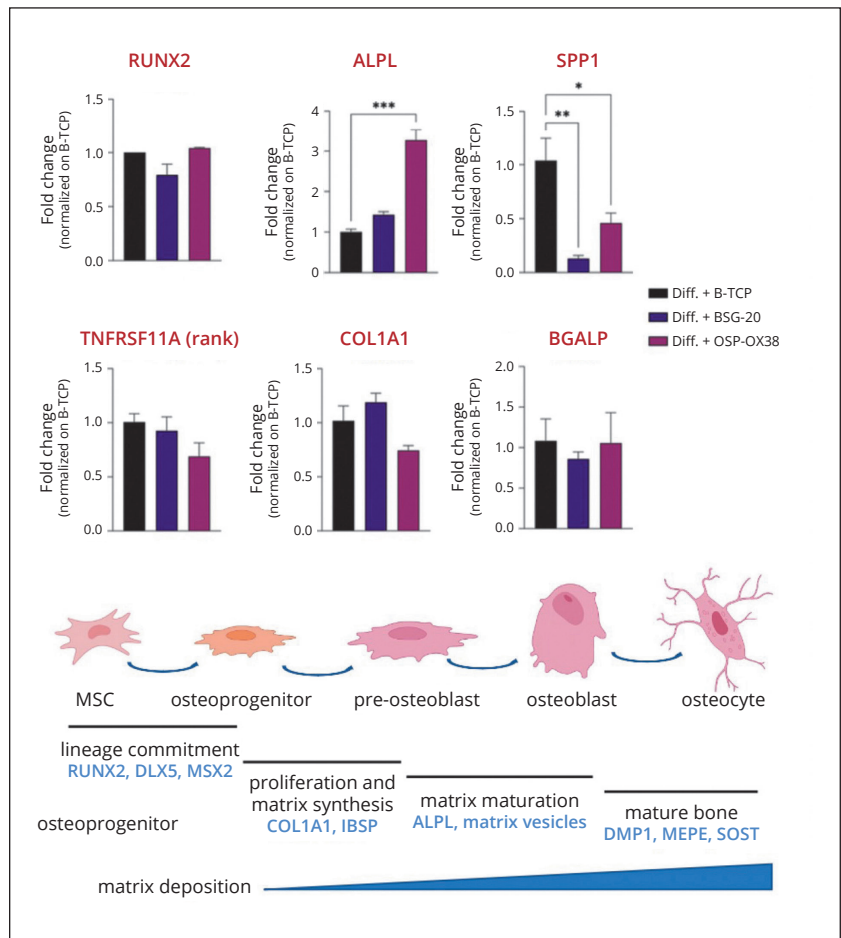
#### Quantitative gene expression analysis with RT-PCR

To further evaluate the osteogenic potential of the biomaterials under investigation, gene expression of the following markers was analyzed after 17 days of incubation in differentiating medium (Figure 10): 1) RUNX2, encoding a nuclear protein with a Runt DNA-binding domain involved in the expression of skeletal genes es-

TABLE I.—Predominant cellular elements observed on the scaffolds during adhesion and osteogenic differentiation experiments.

	Cell adhesion (day 3)	Cell adhesion (day 10)	Osteogenic differentiation (day 17)	
			Non-induced	Induced
EBHC	Inter-granule tissue fibers	Inter-granule tissue fibers	NFR-positive tissue fibers	NFR-positive tissue fibers
EBPC	Single cells	Tissue covering the scaffold surface	NFR-positive tissue fibers VK-positive deposits	NFR-positive tissue fibers VK-positive deposits
β-TCP	Single cells	Single cells	VK-positive deposits	VK-positive deposits

Figure 10.—Different gene expression profiles were observed across the three biomaterials tested. Gene expression analysis of 143B cells on β-TCP, EBHC, and EBPC (N.=3 per group), performed 17 days after induction of differentiation. All data were normalized to the respective GAPDH expression and expressed as fold change relative to β-TCP results (mean±SEM). Statistical analysis was performed using one-way ANOVA followed by Dunnett’s multiple comparison test (ALPL—EBPC OSP-OX38 vs. β-TCP P=0.0001; SPP1—EBHC BSG-20 vs. β-TCP P=0.0051, EBPC OSP-OX38 vs. β-TCP P=0.037). (B) Graphical scheme illustrating the expression of osteogenic differentiation markers. \*\*\*P<0.001, \*\*P<0.01, \*P<0.05.



essential for osteoblastic differentiation and skeletal morphogenesis; 2) ALPL, encoding alkaline phosphatase, an enzyme involved in bone mineralization; 3) SPP1, encoding osteopontin, which is involved in the attachment of osteoclasts to the mineralized bone matrix; 4) TNFRSF11A (RANK), a member of the TNF receptor superfamily that interacts with various TRAF family proteins and triggers activation of NF-κB and MAPK8/JNK, critical for osteoclast develop-

ment; 5) COL1A1, encoding type I fibril-forming collagen found in most connective tissues and abundant in bone; 6) BGLAP, encoding osteocalcin, a highly abundant bone protein secreted by osteoblasts that regulates bone remodeling. RT-PCR analysis showed a statistically significant higher level of ALPL and a lower level of SPP1 in the presence of EBPC compared to β-TCP. A significantly lower level of SPP1 was also observed with EBHC compared to β-TCP.

No significant differences were found in the expression of the other examined genes (RUNX2, TNFRSF11A, COL1A1, and BGLAP).

### Discussion

In dental surgery, as well as in orthopedics and neurosurgery, bone defects represent a significant clinical challenge in daily practice. Advances in bone grafting materials have demonstrated their ability to control bone regeneration, reduce the risk of disease transmission, and accelerate healing.<sup>2, 3, 5, 36, 37</sup> Due to the morphological and compositional similarities between human bone minerals and those of other mammals, xenografts produced by processing heterologous bones to make them non-antigenic appear very promising. Among xenografts, recent studies have suggested the use of enzyme-deantigenized equine bone containing type I bone collagen in various clinical contexts as an alternative to other materials.<sup>23-27, 33-35, 38</sup> Notably, the efficacy of EBPC has been histomorphometrically evaluated in bone samples following sinus augmentation procedures. Results indicate a higher amount of newly formed bone in the EBPC-treated group, alongside a smaller quantity of residual biomaterial compared to groups treated with anorganic bovine bone.<sup>34</sup> These findings align with other histological studies on maxillary sinus augmentation, demonstrating new bone formation as early as three months post-surgery.<sup>33</sup> Similarly, in post-extraction socket procedures, restoring alveolar bone at the tooth extraction site is essential to prevent alveolar bone resorption, as shown by Di Stefano *et al.*<sup>35</sup> Their study compared collagen-free materials to EBPC and highlighted how EBPC, which preserves collagen in its native state, facilitates faster and greater new bone formation. EBHC has also been histologically evaluated in various studies.<sup>39-41</sup> In bone defects of the alveolar processes of the maxilla and mandible, EBHC showed a slight but statistically significant increase in optical density compared to other collagen-free xenografts.<sup>41</sup> Moreover, in sinus augmentation, the high percentage of regenerated bone suggests that EBHC can be resorbed within six months and likely replaced by newly formed vital bone.<sup>40</sup> Building on this evi-

dence, further investigation at the cellular level was needed to better understand these processes.

Here, we evaluated the *in vitro* properties of two bone substitutes: EBHC, containing hydrolyzed type I collagen, and EBPC, containing preserved type I collagen, comparing both to  $\beta$ -TCP, one of the most commonly used synthetic bone substitutes.<sup>42</sup> Our study demonstrates that all three bone graft substitutes exhibit good and comparable biocompatibility. However, they differ in their ability to support matrix deposition, a critical process for new bone formation.<sup>43</sup> Cells grown with  $\beta$ -TCP showed a complete absence of intergranular tissue fibers or matrix, both before and after osteogenic differentiation. In contrast, cells seeded on EBHC developed intergranular tissue fibers. EBPC performed even better, with the presence of single cells and matrix observed not only after differentiation but also in non-differentiated cultures, suggesting that cells on this substitute may have an inherent ability to differentiate (Figure 2, 3).

These observations are further supported by our gene expression analysis of markers involved in bone remodeling (Figure 10). Bone homeostasis is maintained by the balanced activity of osteoblasts and osteoclasts, through the interplay of osteoclast-mediated bone resorption and osteoblast-mediated bone formation.<sup>44</sup> The ALPL gene encodes alkaline phosphatase, an enzyme highly expressed in osteoblasts that hydrolyzes inorganic pyrophosphate, a calcification inhibitor, thus lowering its concentration and promoting calcification and bone formation.<sup>45</sup> The SPP1 gene encodes osteopontin, a protein involved in osteoclastogenesis and osteoclast-mediated bone resorption.<sup>46</sup> The finding that cells grown on EBPC express high levels of ALPL but low levels of SPP1 suggests that this biomaterial's superior performance may be due to its ability to facilitate faster bone mineralization. Conversely,  $\beta$ -TCP's poor performance could be related to enhanced bone resorption, as indicated by the highest SPP1 and lowest ALPL levels. Cells cultured with EBHC showed the lowest SPP1 levels but also low ALPL levels, suggesting an intermediate performance, with bone mineralization kinetics faster than  $\beta$ -TCP but slower than EBPC. It is important to note, however, that dif-

ferent dynamics might occur beyond the 17-day differentiation period analyzed here. Previous studies<sup>47</sup> have shown that longer culture times may be needed to detect increases in ALPL and other genes. A detailed analysis of the secretome from cells grown on the three scaffolds, measuring proteins involved in matrix mineralization over time, would help clarify these differences.

Ideally, a scaffold should mimic natural bone properties, providing both the biochemical environment and biomechanical support necessary for bone formation. The bone matrix, composed of organic and inorganic components, is crucial in bone tissue engineering.<sup>48</sup> Another *in vitro* study<sup>49</sup> examined how thermal processing of bovine-derived hydroxyapatite scaffolds at temperatures from 100-220 °C up to 300-500 °C affects their interactions with osteoclasts and osteoblasts. Results showed that increasing temperature progressively reduced the scaffolds' ability to support effective cell-material interactions. Notably, most commercial heterologous biomaterials undergo much higher temperature processing (600-1400 °C)<sup>49</sup>. In that study, scaffolds treated at 130 °C and 160 °C demonstrated the best biological responses, including enhanced osteoblast proliferation, higher alkaline phosphatase activity, and increased expression of osteogenic genes. Preservation of the bone's natural surface morphology was also emphasized as a key factor for cell attachment *in vitro*.<sup>49</sup> Given the close link between material properties and microstructure, EBHC and EBPC appear advantageous because they maintain their native structure and surface, essential for predictable biological outcomes and complete integration through physiological resorption.<sup>50, 51</sup> EBPC, in particular, retains its native collagen structure, fully expressing its biological potential. This structural integrity supports rapid remodeling, promoting new bone formation alongside gradual biomaterial degradation.<sup>34, 35</sup> At the cellular level, EBPC maintains a physiological balance between osteoclast and osteoblast activity, enabling natural resorption aligned with the body's remodeling process.

In contrast, EBHC shows a different biological response. It stimulates osteoblast activity more than  $\beta$ -TCP, but less than EBPC, leading to slower remodeling and persistence of biomate-

rial residues. EBHC also shows predominant osteoclast activity compared to  $\beta$ -TCP and EBPC.

Moreover, unlike thermally treated xenografts and synthetic substitutes like  $\beta$ -TCP, EBPC and EBHC are derived from equine bone processed enzymatically to eliminate immunogenicity while preserving the extracellular matrix and bone collagen without accumulating harmful chemical residues. Extending previous observations,<sup>31-35</sup> our results indicate that the enzyme-based production and presence of type I collagen are key factors enhancing bone matrix deposition. The extent of this improvement depends on whether the collagen is native or hydrolyzed. Clinically, these findings suggest that, compared to  $\beta$ -TCP, EBHC may be better suited for small, contained defects where slower resorption is acceptable, while EBPC may be preferable for larger or less contained defects where favorable biological conditions for bone deposition are needed.

Nevertheless, clinicians should base their decisions on a comprehensive assessment of each patient's specific needs and medical conditions. The evaluation of a single timepoint after cell differentiation induction (*i.e.*, 17 days) represents a main limitation of this study, as it prevents investigation of both early and late gene expression dynamics. Similarly, cell adhesion and viability on scaffolds – assessed here at days 3 and 10 after seeding – should also be evaluated at additional timepoints. Although the granule size used (0.25-1 mm) falls within the commonly used range for bone graft substitutes, its potential influence on cell attachment, proliferation, and differentiation should be considered, since microstructural features can significantly affect cellular behavior.

In addition, the use of a single cell line (143B) limits the generalizability of the findings, as it may not fully reflect the responses of primary human osteoblasts or other relevant cell types – an important factor for clinical translation. Therefore, conducting further experiments using additional cell lines, ideally closely resembling human cells of interest, would be valuable. Future studies will aim to evaluate the osteogenic potential of the biomaterials, as well as cell adhesion and viability on scaffolds, at multiple timepoints.

Finally, since the presence of BMPs in these biomaterials remains unknown, a promising direction for future research would be to investigate whether such proteins are present and evaluate their possible biological impact.<sup>52</sup>

### Conclusions

Despite its relatively simple structure – comprising three types of cell subpopulations, an organic phase mainly composed of collagen, and an inorganic phase primarily made of hydroxyapatite – the complex regulation of bone metabolism poses a significant challenge in developing an “ideal” substitute material. Understanding the intricate interactions between biomaterials and bone components is essential for creating new substitutes that support this synergy and promote healing and repair.

Both collagen-containing bone xenografts evaluated in this study demonstrated high biocompatibility and the ability to support osteogenic differentiation, with EBPC showing greater effectiveness in matrix deposition compared to EBHC. While the notion of a universally ideal bone substitute is appealing, it is more realistic to assume that the choice of biomaterial should be dictated by the specific clinical application.

This study offers important insights to help oral surgeons make informed decisions, particularly by emphasizing the role of natural remodeling kinetics in bone regeneration procedures for implant placement. A biomaterial containing preserved collagen and exhibiting physiological remodeling kinetics offers a dual benefit: it promotes early-stage new bone deposition – supporting successful osseointegration and volume preservation – and it allows for complete replacement by the patient’s own vital bone within a physiological timeframe. This makes it particularly suitable for cases requiring full remodeling, rapid integration, and the eventual absence of residual biomaterial. In turn, this may help reduce the risk of peri-implantitis progression, as inert residues can serve as a substrate for bacterial colonization in rare cases where infection develops.

In contrast, in cases of small or localized defects, a biomaterial containing hydrolyzed collagen may offer an effective solution, with slower

remodeling that may be clinically acceptable or even preferable.

While these findings provide valuable guidance for surgeons, further research is essential to refine biomaterial selection and ensure optimal outcomes tailored to each patient’s specific clinical scenario.

### References

1. Abtahi S, Chen X, Shahabi S, Nasiri N. Resorbable Membranes for Guided Bone Regeneration: Critical Features, Potentials, and Limitations. *ACS Mater Au* 2023;3:394–417.
2. Fillingham Y, Jacobs J. Bone grafts and their substitutes. *Bone Joint J* 2016;98-B(Suppl A):6–9.
3. Bhatt RA, Rozental TD. Bone graft substitutes. *Hand Clin* 2012;28:457–68.
4. Elsalanty ME, Genecov DG. Bone grafts in craniofacial surgery. *Craniofacial Trauma Reconstr* 2009;2:125–34.
5. Kao ST, Scott DD. A review of bone substitutes. *Oral Maxillofac Surg Clin North Am* 2007;19:513–21, vi.
6. Misch CE, Dietsch F. Bone-grafting materials in implant dentistry. *Implant Dent* 1993;2:158–67.
7. Bauer TW, Muschler GF. Bone graft materials. An overview of the basic science. *Clin Orthop Relat Res* 2000;(371):10–27.
8. Haugen HJ, Lyngstadaas SP, Rossi F, Perale G. Bone grafts: which is the ideal biomaterial? *J Clin Periodontol* 2019;46(Suppl 21):92–102.
9. Roberts TT, Rosenbaum AJ. Bone grafts, bone substitutes and orthobiologics: the bridge between basic science and clinical advancements in fracture healing. *Organogenesis* 2012;8:114–24.
10. Yazdi FK, Mostaghni E, Moghadam SA, Faghihi S, Monabati A, Amid R. A comparison of the healing capabilities of various grafting materials in critical-size defects in guinea pig calvaria. *Int J Oral Maxillofac Implants* 2013;28:1370–6.
11. Oryan A, Alidadi S, Moshiri A, Maffulli N. Bone regenerative medicine: classic options, novel strategies, and future directions. *J Orthop Surg Res* 2014;9:18.
12. Benefits and associated risks of using allograft, autograft and synthetic bone fusion material for patients and service providers - A Systematic Review. *JBIR Library of Systematic Reviews* 2010;8:1-13.
13. Kurkcu M, Benlidayi ME, Cam B, Sertdemir Y. Anorganic bovine-derived hydroxyapatite vs  $\beta$ -tricalcium phosphate in sinus augmentation: a comparative histomorphometric study. *J Oral Implantol* 2012;38(S1):519–26.
14. Schwartz Z, Doukarsky-Marx T, Nasatzky E, Goultschin J, Ranly DM, Greenspan DC, *et al.* Differential effects of bone graft substitutes on regeneration of bone marrow. *Clin Oral Implants Res* 2008;19:1233–45.
15. Zecha PJ, Schortinghuis J, van der Wal JE, Nagursky H, van den Broek KC, Sauerbier S, *et al.* Applicability of equine hydroxyapatite collagen (eHAC) bone blocks for lateral augmentation of the alveolar crest. A histological and histomorphometric analysis in rats. *Int J Oral Maxillofac Implants* 2011;40:533–42.
16. Benke D, Olah A, Möhler H. Protein-chemical analysis of Bio-Oss bone substitute and evidence on its carbonate content. *Biomaterials* 2001;22:1005–12.

17. Kim Y, Nowzari H, Rich SK. Risk of prion disease transmission through bovine-derived bone substitutes: a systematic review. *Clin Implant Dent Relat Res* 2013;15:645–53.
18. Canullo L, Del Fabbro M, Khijmatgar S, Panda S, Ravidà A, Tommasato G, *et al.* Dimensional and histomorphometric evaluation of biomaterials used for alveolar ridge preservation: a systematic review and network meta-analysis. *Clin Oral Investig* 2022;26:141–58.
19. Caiazzo A, Canullo L, Pesce P, Pesce P; Consensus Meeting Group. Consensus Report by the Italian Academy of Osseointegration on the Use of Graft Materials in Postextraction Sites. *Int J Oral Maxillofac Implants* 2022;37:98–102.
20. Colaço HB, Shah Z, Back D, Davies A, Ajuied A 4th. Xenograft in orthopaedics. *Orthop Trauma* 2015;29:253–60.
21. Stogov MV, Smolentsev DV, Kireeva EA. Bone Xenografts in Trauma and Orthopaedics (Analytical Review). *Traumatology and Orthopedics of Russia* 2019;26:181-9.
22. Ferraz MP. Bone Grafts in Dental Medicine: An Overview of Autografts, Allografts and Synthetic Materials. *Materials (Basel)* 2023;16:4117.
23. Rollo G, Prkic A, Bisaccia M, Eygendaal D, Pichierrri P, Marsilio A, *et al.* Grafting and fixation after aseptic non-union of the humeral shaft: A case series. *J Clin Orthop Trauma* 2020;11(Suppl 1):S51–5.
24. Rollo G, Luceri F, Bisaccia M, Lanzetti RM, Luceri A, Agnoletto M, *et al.* Allograft versus autograft in forearm aseptic non-union treatment. *J Biol Regul Homeost Agents* 2020;34(Suppl. 3):207–12.
25. Piolanti N, Del Chiaro A, Matassi F, Nistri L, Graceffa A, Marcucci M. Bone integration in acetabular revision hip arthroplasty using equine-derived bone grafts: a retrospective study. *Eur J Orthop Surg Traumatol* 2019;31858258.
26. Sonmez MM, Armagan R, Ugurlar M, Eren T. Allografts versus Equine Xenografts in Calcaneal Fracture Repair. *J Foot Ankle Surg* 2017;56:510–3.
27. Stievano D, Di Stefano A, Ludovichetti M, Pagnutti S, Gazzola F, Boato C, *et al.* Maxillary sinus lift through heterologous bone grafts and simultaneous acid-etched implants placement. Five year follow-up. *Minerva Chir* 2008;63:79–91.
28. Mattioli B, Iacoviello P, Aldiano C, Verrina G. Subcranial Le Fort III advancement with equine-derived bone grafts to correct syndromic midfacial hypoplasia: a case report. *J Maxillofac Oral Surg* 2018;17:296–300.
29. Campana V, Milano G, Pagano E, Barba M, Cicione C, Salonna G, *et al.* Bone substitutes in orthopaedic surgery: from basic science to clinical practice. *J Mater Sci Mater Med* 2014;25:2445–61.
30. Georgeanu VA, Gingu O, Antoniac IV, Manolea HO. Current Options and Future Perspectives on Bone Graft and Biomaterials Substitutes for Bone Repair, from Clinical Needs to Advanced Biomaterials Research. *Appl Sci (Basel)* 2023;13:8471.
31. Perrotti V, Nicholls BM, Piattelli A. Human osteoclast formation and activity on an equine spongy bone substitute. *Clin Oral Implants Res* 2009;20:17–23.
32. Perrotti V, Nicholls BM, Horton MA, Piattelli A. Human osteoclast formation and activity on a xenogenous bone mineral. *J Biomed Mater Res A* 2009;90:238–46.
33. Di Stefano DA, Gastaldi G, Vinci R, Polizzi EM, Cinci L, Pieri L, *et al.* Bone formation following sinus augmentation with an equine-derived bone graft: a retrospective histological and histomorphometric study with 36-month follow-up. *Int J Oral Maxillofac Implants* 2016;31:406–12.
34. Di Stefano DA, Gastaldi G, Vinci R, Cinci L, Pieri L, Gherlone E. Histomorphometric comparison of enzyme-deantigenic equine bone and anorganic bovine bone in sinus augmentation: a randomized clinical trial with 3-year follow-up. *Int J Oral Maxillofac Implants* 2015;30:1161–7.
35. Di Stefano DA, Zaniol T, Cinci L, Pieri L. Chemical, Clinical and Histomorphometric Comparison between Equine Bone Manufactured through Enzymatic Antigen-Elimination and Bovine Bone Made Non-Antigenic Using a High-Temperature Process in Post-Extractive Socket Grafting. A Comparative Retrospective Clinical Study. *Dent J* 2019;7:70.
36. Fernandez de Grado G, Keller L, Idoux-Gillet Y, Wagner Q, Musset AM, Benkirane-Jessel N, *et al.* Bone substitutes: a review of their characteristics, clinical use, and perspectives for large bone defects management. *J Tissue Eng* 2018;9:2041731418776819.
37. Wang W, Yeung KW. Bone grafts and biomaterials substitutes for bone defect repair: A review. *Bioact Mater* 2017;2:224–47.
38. Pistilli R, Signorini L, Pisacane A, Lizio G, Felice P. Case of severe bone atrophy of the posterior maxilla rehabilitated with blocks of equine origin bone: histological results. *Implant Dent* 2013;22:8–15.
39. Grasso G, Mummolo S, Bernardi S, Pietropaoli D, D’Ambrosio G, Iezzi G, *et al.* Histological and Histomorphometric Evaluation of New Bone Formation after Maxillary Sinus Augmentation with Two Different Osteoconductive Materials: A Randomized, Parallel, Double-Blind Clinical Trial. *Materials (Basel)* 2020;13:5520.
40. Rivara F, Negri M, Lumetti S, Parisi L, Toffoli A, Calciolari E, *et al.* Maxillary sinus floor augmentation using an equine-derived graft material: preliminary results in 17 patients. *BioMed Res Int* 2017;2017:9164156.
41. Śmieszek-Wilczewska J, Koszowski R, Pająk J. Comparison of postoperation bone defects healing of alveolar processes of maxilla and mandible with the use of Bio-Gen and Bio-Oss. *J Clin Exp Dent* 2010;2:60–6.
42. Bohner M, Santoni BL, Döbelin N.  $\beta$ -tricalcium phosphate for bone substitution: synthesis and properties. *Acta Biomater* 2020;113:23–41.
43. Lin X, Patil S, Gao YG, Qian A. The Bone Extracellular Matrix in Bone Formation and Regeneration. *Front Pharmacol* 2020;11:757.
44. Faqeer A, Wang M, Alam G, Padhiar AA, Zheng D, Luo Z, *et al.* Cleaved SPP1-rich extracellular vesicles from osteoclasts promote bone regeneration via TGF $\beta$ 1/SMAD3 signaling. *Biomaterials* 2023;303:122367.
45. Nakamura T, Nakamura-Takahashi A, Kasahara M, Yamaguchi A, Azuma T. Tissue-nonspecific alkaline phosphatase promotes the osteogenic differentiation of osteoprogenitor cells. *Biochem Biophys Res Commun* 2020;524:702–9.
46. Boyle WJ, Simonet WS, Lacey DL. Osteoclast differentiation and activation. *Nature* 2003;423:337–42.
47. Foschi F, Conserva E, Pera P, Canciani B, Cancedda R, Mastrogiacomo M. Graft materials and bone marrow stromal cells in bone tissue engineering. *J Biomater Appl* 2012;26:1035–49.
48. Ravindran S, Gao Q, Kotecha M, Magin RL, Karol S, Bedran-Russo A, *et al.* Biomimetic extracellular matrix-incorporated scaffold induces osteogenic gene expression in human marrow stromal cells. *Tissue Eng Part A* 2012;18:295–309.
49. Porter GC, Abdelmoneim D, Li KC, Duncan WJ, Coates DE. The Effect of Low-Temperature Thermal Processing on Bovine Hydroxyapatite Bone Substitutes, toward Bone Cell Interaction and Differentiation. *Materials (Basel)* 2022;15:2504.

**50.** Falvo D'Urso Labate G, Baino F, Terzini M, Audenino A, Vitale-Brovarone C, Segers P, *et al.* Bone structural similarity score: a multiparametric tool to match properties of biomimetic bone substitutes with their target tissues. *J Appl Biomater Funct Mater* 2016;14:e277–89.

**51.** Bedini R, Pecci R, Meleo D, Campioni I. Bone Substi-

tutes Scaffold in Human Bone: Comparative Evaluation by 3D Micro-CT Technique. *Appl Sci (Basel)* 2020;10:3451.

**52.** Cicciù M, Fiorillo L, Cervino G, Habal MB. Bone Morphogenetic Protein Application as Grafting Materials for Bone Regeneration in Craniofacial Surgery: Current Application and Future Directions. *J Craniofac Surg* 2021;32:787–93.

---

#### *Conflicts of interest*

Matteo Colombo, Christian Frigerio, Anna Di Bona, Daniele Recupero and Marco Morroni work for Bioteck S.p.A.

#### *Funding*

The research was funded by Bioteck S.p.A.

#### *Authors' contributions*

All authors read and approved the final version of the manuscript.

#### *Acknowledgments*

Paolo Capparè, beloved friend and insightful researcher. We had begun this research with him when he prematurely passed away. This work is dedicated to him. We thank Elena Veronesi, for her support in the setting-up of the microscopic analysis and Stefano Pagnutti, for his support in study design.

#### *History*

Article first published online: October 28, 2025. - Manuscript accepted: July 15, 2025. - Manuscript revised: June 26, 2025. - Manuscript received: April 10, 2025.